

Open Access Article

X-RAY DIFFRACTION ANALYSIS OF GREEN SYNTHESIZED ZINC OXIDE NANOCRYSTALLITES USING WAVELET DENOISING

Ravikant Divakar

Department of Physics, Hindu College, Moradabad, U.P. (INDIA)

Anil Kumar

Department of Physics, Hindu College, Moradabad, U.P. (INDIA)

Email: akumarmbd@gmail.com

Abstract: The zinc oxide (ZnO) nanocrystallites are synthesized from zinc nitrate hexahydrate by a sol-gel combustion process using aloe-vera gel. As prepared ZnO nanocrystallites are characterized using X-ray diffraction (XRD). In wavelet analysis, a suitable wavelet is selected for a given signal and its wavelet coefficients are determined. Thresholding of wavelet coefficients is performed to zero out small magnitude coefficients and retain the large magnitude coefficients. X-ray diffractogram is denoised through discrete wavelet transform's soft Thresholding. In denoised signals clear and sharp peaks are observed. X-ray diffraction study confirms the crystalline nature of ZnO nanocrystallites. The diffraction peaks become sharper with increasing calcination temperature indicating the enhancement of crystallinity.

Keywords: Zinc oxide, nanocrystallite, green synthesis, XRD, wavelet transform, denoising

【摘要】：以六水硝酸锌为原料,采用芦荟凝胶溶胶 凝胶燃烧法合成氧化锌(ZnO)纳米晶。所制备的 ZnO 纳米微晶使用 X 射线衍射 (XRD) 进行表征。在小波分析中,为给定信号选择合适的小波并确定其小波系数。执行小波系数的阈值处理以将小幅度系数清零并保留大幅度系数。射线衍射图通过离散小波变换的软阈值去噪。在去噪信号中观察到清晰且尖锐的峰。X 射线衍射研究证实了 ZnO 纳米微晶的结晶性质。随着煅烧温度的升高,衍射峰变得更尖锐,表明结晶度提高。

关键词：氧化锌, 纳米微晶, 绿色合成, XRD, 小波变换, 去噪

1. Introduction

The inorganic metal oxide nanocrystallites have attracted considerable attention in physical,

chemical, biological, medical, and engineering sciences where innovative synthesis techniques are being developed to explore and manipulate

Received: March 7, 2021 / Revised: April 19, 2021 / Accepted: May 11, 2021 / Published: June 18, 2021

About the authors: Ravikant Divakar, Department of Physics, Hindu College, Moradabad, U.P. (INDIA)

Corresponding author Email: Anil Kumar, Email: akumarmbd@gmail.com

single atoms and molecules [1]. The green synthesized metallic oxide nanocrystallites are eco-friendly, cheap, fast and have a renewable approach. The green synthesis is an ecological and safe technique because it is performed at low temperature [2-3]. ZnO nanocrystallites act as smart material towards multidrug-resistant microorganisms and an intelligent substitute approach to antibiotics. Due to the high surface to volume ratio of metal and metal oxide nanoparticles they possess catalytic, antimicrobial, magnetic, and electronic activity. The properties of nanocrystallites depend on their composition, size, shape, morphology and crystalline phase. Due to the smaller size of nanoparticles, their movement is mainly governed by Brownian motion and the gravity effect is negligible. Nanoparticles are able to overcome physiological barriers and readily interact with intracellular compartments without any additional surgery [4].

Fourier transform has been an important analytical tool to analyse data/signals. The main drawback of Fourier transform is that this can be applicable only on stationary signals or data [5]. In window Fourier transform (WFT), a window function depending upon signal is taken in place of exponential function and then transformation is performed. In WFT, the product in time resolution and frequency resolution are restricted by Heisenberg uncertainty principle, hence can not be arbitrarily small simultaneously. The wavelet transform overcomes the shortcomings of Fourier and window Fourier transforms in analysis of non-stationary signals/data. Wavelets belonging to a family are generated by a single function called mother wavelet. The literal meaning of wavelet is small wave, which

grows from zero reaches maximum and decreases back to zero such that average displacement is zero [6]. Therefore, we can say that a wavelet has a location where it maximizes, a characteristic time period and a scale where it amplifies and declines. The wavelet theory provides a new analytical concept in the field of non-stationary and chaotic data analysis. It reveals the average and differential behaviour of a signal successively. Therefore, the wavelet analysis has been widely used in data processing algorithms in X-ray crystallography and several other branches of the physical sciences.

In x-ray diffraction crystallography, wavelet-based data analysis is being employed to X-ray diffraction patterns to improve both computation efficiency and identify crystalline phases. The wavelet denoising algorithms demonstrate high sensitivity and low false detection rate for peak identification in XRD pattern [7]. We demonstrate successful analysis of diffraction patterns of green synthesized ZnO nanocrystallites. The Bragg peaks are efficiently analyzed via the algorithms described in the paper.

2. Wavelet transforms and denoising

A mother function is used to generate a whole family of wavelets using dilation and translation:-

$$\Psi_{a,b}(x) = \frac{1}{\sqrt{a}} \psi\left(\frac{x-b}{a}\right) = T_b D_a \psi \quad (1.1)$$

where a is the dialation or scaling parameter, b is the translation parameter and $\psi(t)$ is real valued function. The continuous wavelet transform of a function f is expressed as:

$$W_{a,b} = \int f(x) \frac{1}{\sqrt{a}} \psi\left(\frac{x-b}{a}\right) dx \quad (1.2)$$

By taking $a = 2^{-j}$ and $b/a = k$ with $j, k \in \mathbb{Z}$, that is, the integers representing the set of discrete dilation and discrete translation, the discrete wavelet transform is defined as [8]:

$$W_{j,k} = \int f(x) 2^{j/2} \psi(2^j x - k) dx \quad (1.3)$$

and discrete wavelets are defined as:

$$\psi_{j,k}(x) = 2^{j/2} \psi(2^j x - k) \quad (1.4)$$

The $\psi_{0,0}(x) = \psi(x)$ is called mother wavelet. The wavelet transforms of a signal capture the localized time frequency information of a signal [2].

2.1 Multi Resolution Analysis (MRA): An MRA is introduced by Mallat and extended by other researchers [9-11] consisting of a sequence $V_j : j \in \mathbb{Z}$ of closed subspaces of Lebesgue space $L^2(\mathbb{R})$, a space of square integrable functions, satisfying the following properties:-

- 1) $V_{j+1} \subset V_j : j \in \mathbb{Z}$
- 2) $\bigcap_{j \in \mathbb{Z}} V_j = \{0\}$, $\bigcup_{j \in \mathbb{Z}} V_j = L^2(\mathbb{R})$,
- 3) For every, $L^2(\mathbb{R}), f(t) \in V_j \Rightarrow f(2t) \in V_{j+1}, \forall j \in \mathbb{Z}$
- 4) There exists a function $\phi(t) \in V_0$, such that $\{\phi(t - k) : k \in \mathbb{Z}\}$ is orthonormal basis of V_0 .

Now we consider W_0 be the orthogonal complement of V_0 in V_1 i.e.

$$V_0 = V_1 \oplus W_1$$

If $\psi \in W_0$ be any function then,

$$\psi(t) = \sum_{k \in \mathbb{Z}} g_k \phi(2t - k)$$

Where $g_k = \left(\frac{1}{\sqrt{2}}\right) \int_{-\infty}^{\infty} \psi(t) \phi(2t - k) dt$ are high pass filters and $g_k = (-1)^{k+1} h_{1-k}$. We can express a signal in terms of bases of V_1 space and W_1 space. If we combine the bases of V_1 and W_1 space, we can express any signal in V_0 space. That is,

$$V_0 = V_1 \oplus W_1$$

In general,

$$V_j = V_{j+1} \oplus W_{j+1} \quad (1.5)$$

But,

$$V_{j+1} = V_{j+2} \oplus W_{j+2}$$

Therefore,

$$V_j = W_{j+1} \oplus W_{j+2} \oplus W_{j+3} \oplus \dots$$

$$V_0 = W_0 \oplus W_1 \oplus W_2 \oplus \dots$$

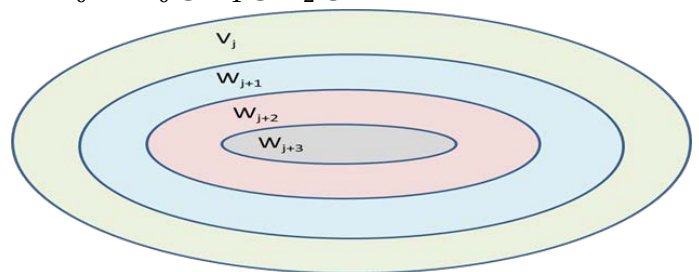


Figure 1: Decomposition of vector space

2.2 Haar Wavelet: Haar discovered the simplest wavelet begins with the function that is equal to 1 on $\left[0, \frac{1}{2}\right]$ and -1 on $\left[\frac{1}{2}, 1\right]$, and 0 outside the interval $[0, 1]$. Haar wavelet is constructed from the multiresolution analysis (MRA) generated by scaling function $\phi(x) = \chi_{[0,1]}(x)$. Since,

$$\phi(x) = \phi(2x) + \phi(2x - 1) = \chi_{[\frac{1}{2}, 1]} + \chi_{[0, \frac{1}{2}]}$$

and

$$\psi(x) = \phi(2x) - \phi(2x - 1) = \chi_{[\frac{1}{2}, 1]} - \chi_{[0, \frac{1}{2}]}$$

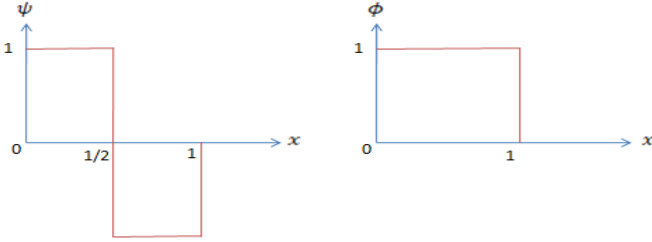


Figure 2: Haar wavelet and its scaling function

2.3 Signal Decomposition: With help of MRA of vector subspaces, a function $f(x)$ can be expressed and decomposed as follows:-

$$\begin{aligned} f(x) &= \sum_{j,k} \langle f, \psi_{j,k} \rangle \psi_{j,k} \\ &= \sum_{j,k} c_{j,k} \psi_{j,k}(x) \end{aligned} \quad (1.6)$$

where $c_{j,k} = \langle f, \psi_{j,k} \rangle$ is called wavelet coefficient [12].

Noise is interpreted as the unwanted, problematic and unavoidable part of any signal. A signal is expressed as,

$$f = f_* + \sigma \cdot \rho \quad (1.7)$$

where f is the noised version of signal f_* , σ is the noise level and ρ is a unit energy noise process. Here signal f_* is coherent with wavelet frame $\psi_{j,k}$ and ρ is non-coherent with respect to frame $\psi_{j,k}$. The coherent signal exhibits a concentration of energy (i.e. localized) in the representation domain and the incoherent signal energy is diffusely spread throughout the representation domain [13].

2.4 Denoising using soft Thresholding

method: In thresholding small magnitude wavelet coefficients become zero out while large magnitude wavelet coefficients are retained [14]. Now we introduce a threshold operator T_γ , defined as:-

$$T_\gamma = F(\mathbb{H}) \rightarrow \ell^2(\mathbb{Z})$$

where $F(\mathbb{H})$ is frame representation operator in Hilbert space \mathbb{H} and $\ell^2(\mathbb{Z})$ is the space of all sequences $\psi_{j,k}$, where $j, k \in \mathbb{Z}$ such that,

$$\sum_{j,k \in \mathbb{Z}} |c_{j,k}|^2 < \infty$$

Soft thresholding method affects the wavelet coefficients greater the threshold level γ , whereas hard thresholding method does not. Soft thresholding is stable and less sensitive for small changes in the signal. Soft Thresholding can be analytically expressed as:-

$$\{T_\gamma\}_{j,k} = \{\text{sign}(c_{j,k}), (|c_{j,k}| - \gamma)\} \quad (1.8)$$

The sub band processing and quantization noise suppression achieved naturally and simultaneously by simply using wavelet frames. Shannon Entropy Cost function is a direct measure of mean square error encountered when the signal is reconstructed using the large magnitude (above threshold) coefficients. That is, the cost function measures how many coefficients are negligible and how many are important in a transformed signal. The basis is called the best basis that concentrates the signal energy over a few coefficients and reveals its time frequency structures. The best basis associated with a signal minimizes the value of Cost function.

3. Materials and method

The present study states a green approach for the synthesis of zinc oxide (ZnO)

nanocrystallites using plant extract of aloe-vera. Aloe-vera gel traps metal ions for synthesizing ZnO nanocrystallite from zinc nitrate hexahydrate. As prepared ZnO nanocrystallites are calcined for 1 hour at temperature 200°C and for 45 minutes at temperature 250°C respectively. The resultant nanocrystallites are characterized using X-ray diffraction (XRD) at a wavelength of 1.5418 Å [15-17]. The above X-ray diffractograms are denoised with the help of discrete wavelet transforms using Haar wavelet [18]. By software dyadwaves we perform soft thresholding of XRD, in which the wavelet coefficients below threshold value ($\gamma = 0.75$) are omitted and wavelet coefficients above threshold value are retained. The inverse wavelet transform of retained wavelet coefficients is performed. In this way, the Denoised X-ray diffraction patterns of the ZnO nanocrystallites are obtained. The reconstructed signal (X-ray diffraction pattern) gives the clear and sharp peaks that can be analyzed in a better way. Block diagram for the denoising process of the XRD signal is shown in figure 3.

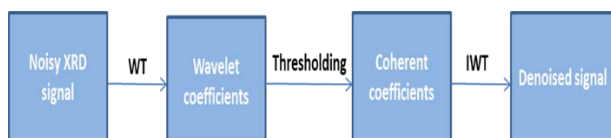


Figure 3: Block diagram for denoising of XRD signal

4. Results and discussion

XRD is performed in the 2θ range of 20-80 degrees at 30kV and 10mA in continuous scanning mode. The XRD patterns of the prepared sample are shown in figure 4. Peaks are observed in figure 4(a), indicating impurities observed in sample calcination at 200°C in a hot air oven. Sharp peaks were found in figure 4

(b), indicating increase in calcination of temperature 250°C in a hot air oven. All detectable peaks are found in standard reference data (JCPDS: 36-1451) [19]. It is clear that diffraction peaks become sharper with increase in calcination temperature indicating the enhancement of crystallinity.

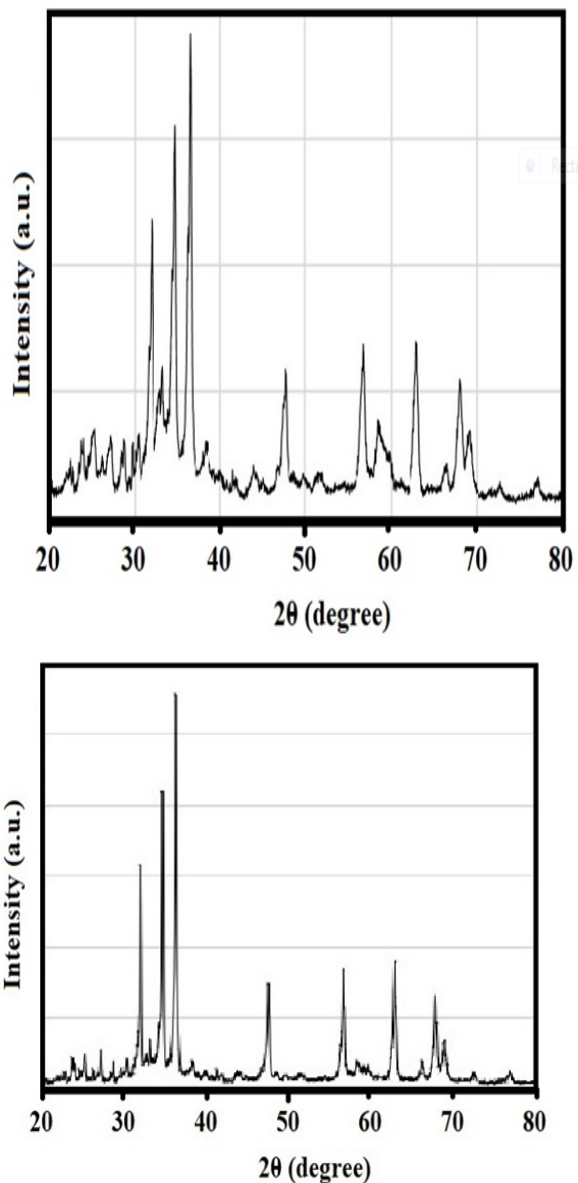


Figure 4: X-ray diffractogram of ZnO nanocrystallites at (a) 200°C (b) 250°C

Open Access Article

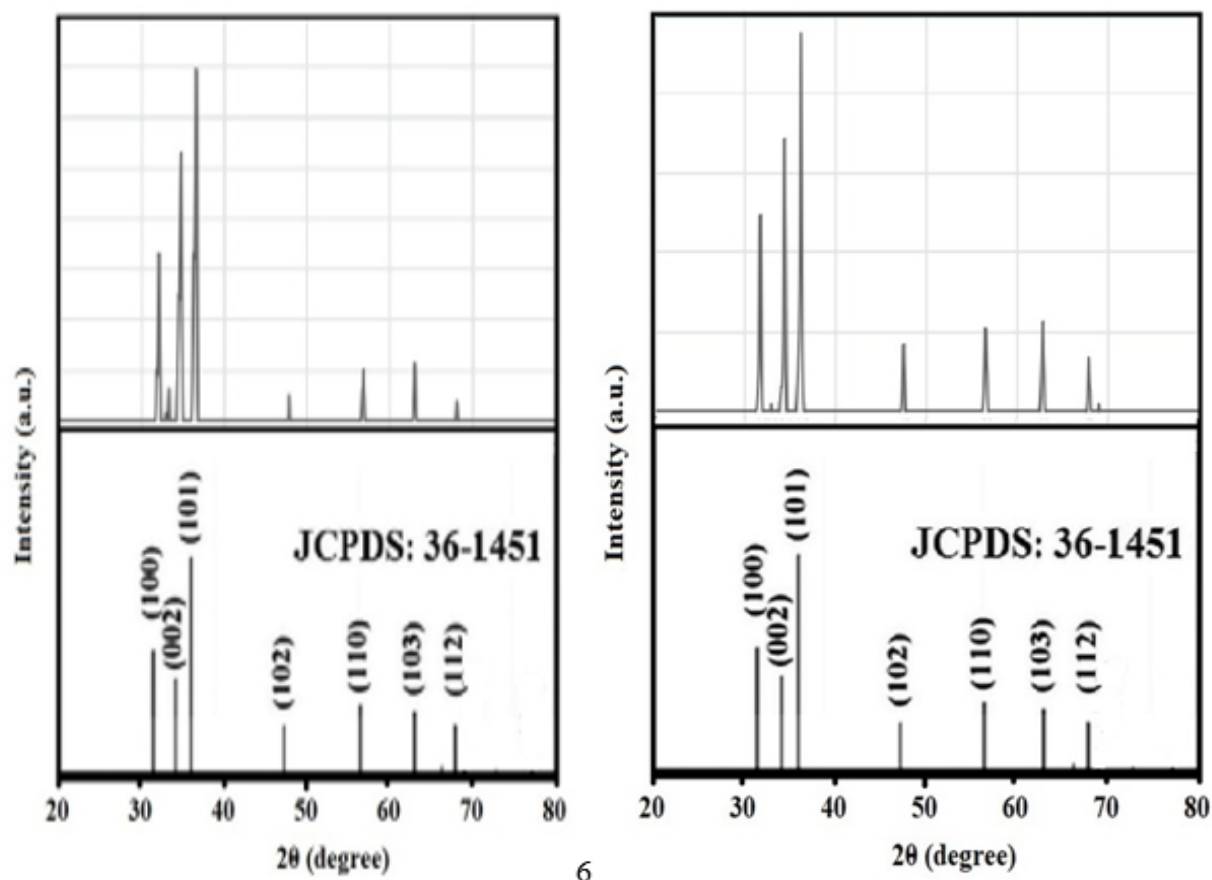


Figure 5: Denoised X-ray diffractogram of ZnO nanocrystallites at a) 200°C (b) 250°C with standard JCPDS: 36-1451

Figure 5: Denoised X-ray diffractogram of ZnO nanocrystallites at a) 200°C (b) 250°C with standard JCPDS: 36-1451

The denoised XRD signals of ZnO nanocrystallites at calcination temperatures 200°C and 250°C are shown in figure 5(a) and 5(b) respectively. The clear and sharp peaks are observed in denoised XRD signals. Diffraction peaks are observed at degrees 31.74, 34.42, 36.21, 47.47, 56.53, 62.77, and 67.81 corresponding to lattice planes (100), (002), (101), (102), (110), (103), (200), and (112) respectively. An additional peak is observed in

the XRD pattern of ZnO nanocrystallite when it is calcined at temperature 200°C (Figure 5(a)). This additional peak represents an impurity in the sample. The peaks are attributed to the hexagonal phase of ZnO (JCPDS file: 36-1451). Crystal lattice indices and particle size can be determined by X-ray diffraction patterns of ZnO nanocrystallites. Interplanar spacing (d) can be determined by Bragg's law:-

$$2d\sin\theta = n\lambda$$

where θ is the Bragg's angle of diffraction, λ is wavelength of X-ray, i.e. $\lambda = 1.5418 \text{ \AA}$ and $n = 1$.

5. Conclusion

ZnO nanocrystallites are synthesized by a sol-gel combustion process using plant extract of aloe-vera as precursor and characterized by powder X-ray diffraction. The wavelet denoised XRD signal shows clear and sharp diffraction peaks. The XRD patterns indicate that ZnO nanocrystallite at higher calcination temperature shows clear and sharp peaks. It is also indicated that higher calcination temperature increases purity and crystallinity of ZnO nanocrystallites. The wavelet denoising algorithm provides a simple and accurate framework for efficiently and precisely analyzing the XRD patterns of nanocrystallites.

References

- [1] L. Theodore, *Nanotechnology: Basic Calculations for Engineers and Scientists*, Wiley, Hoboken, 2006.
- [2] S. Ahmed, A. Saif, A. Chaudhary and A. Ikram, A review on biogenic synthesis of ZnO nano particle using plant extracts and microbes: A prospect toward Green Chemistry, *Journal of Photochemistry and Photobiology B*, 166, 2017, 272-284
- [3] H. Mirzaei and M. Darroudi, Zinc oxide nanoparticles: biological synthesis and biomedical applications, *Ceram. Int*, 43, 2017, 907–914
- [4] R. Seshadari, C.N.R. Rao, A. Muller and A.K. Cheetham (Eds.), *The Chemistry of Nanomaterials*, Wiley-VCH Verlag GmbH, 1, 2010, 94-112.
- [5] D. Kammler, *A first course of Fourier Analysis*, Prentice-Hall, 2000.
- [6] C.K. Chui, *An Introduction Wavelets*, Academic Press, New York 1992.
- [7] John M. Gregoire, Darren Dale and R. Bruce van Dover, A wavelet transform algorithm for peak detection and application to powder X-ray diffraction data, *Review of Scientific Instruments*, 82, 2011, 015105-(1-8)
- [8] J.P. Antoine, “Wavelet analysis: A new tool in Physics”, *Wavelets in Physics* (Van Den Berg, J. C., ed.), 2004, 9-21.
- [9] S.G. Mallat, Multiresolution approximations and wavelet orthonormal bases of $L^2(\mathbb{R})$, *Trans. Amer. Math. Soc.*, 315, 1989, 69-87.
- [10] I. Daubechies, The wavelet transform, time frequency localization and signal analysis, *IEEE Trans. Inform. Theory*, Vol. 36, 1990, 961-1005.
- [11] A. Cohen, I. Daubechies and P. Vial, Wavelets on the interval and fast algorithms, *Journal of Applied and Computational Harmonic Analysis*, 1, 1993, 54-81.
- [12] A. Grossmann, J. Morlet, and T. Paul “Transforms associated to square integrable group representation”, *Journal of Mathematical Physics*, 26, 1985, 2473-2579.
- [13] L. Jhang, X. Wu, P. Bao, Noisy signal compression by wavelet transform with optimal down sampling, *International Journal of Wavelets, Multiresolution and Information Processing*, 1(4), 2003, 407-427.
- [14] N.D. Pah and D.K. Kumar, “Thresholding wavelet network for signal classification” *International Journal of Wavelets, Multiresolution and Information Processing*, 1(3), 2003, 243-261.
- [15] D. Gnanasangeetha and S. Thambavani, One pot synthesis of zinc oxide

-
- nanoparticles via chemical and green method, *Res J Material Sci*, 1, 2013, 1-8.
- [16] P. Vanathi, P. Rajiv, S. Narendhran, S. Rajeshwari and P.K.S.M. Rahman, Biosynthesis and characterization of phyto mediated zinc oxide nanoparticles: a green chemistry approach, *Mater. Lett*, Vol. 134, 2014, 13–15.
- [17] M. Stan, A. Popa, D. Toloman, A. Dehelean, I. Lung and G. Katona, Enhanced photocatalytic degradation properties of zinc oxide nanoparticles synthesized by using plant extracts, *Mater. Sci. Semicond. Process*, 39, 2015, 23–29.
- [18] A. Kumar, Selection of optimal base wavelet for image compression, *World Journal of Engineering Research and Technology*, 3(4), 2017, 396-405.
- [19] M. Anbuvaran, M. Ramesh, G. Viruthagiri, N. Shanmugam and N. Kannadasan, Synthesis, characterization and photocatalytic activity of ZnO nanoparticles prepared by biological method, *Spectrochim., Acta A Mol. Biomol. Spectrosc*, 143, 2015, 304–308.